ISSN 0023-1584, Kinetics and Catalysis, 2010, Vol. 51, No. 4, pp. 602–608. © Pleiades Publishing, Ltd., 2010.

Catalytic Activity of Palladium Supported on Mesoporous Modified Y-Zeolite in Methane Combustion[1]

H. Najar, M. Saïd Zina, and A. Ghorbel

Laboratoire de Chimie des Matériaux et Catalyse, Faculté des Sciences de Tunis, Université El-Manar, Tunisie

e-mail: hanene.naj@gmail.com

Received May 13, 2009

Abstract—Palladium-based catalysts were prepared by the ion-exchange method with dealuminated HY zeolite as support. The support dealumination was realised using acid solution of HNO_3, HCl or H_2SiF_6. The high activity of prepared catalysts for methane combustion was observed. This activity was dependent on the Al concentration, structural and textural properties of the support changed after the dealumination. Especially, Pd loaded on supports developing a second pore system, and having the highest Si/Al ratio, was more active than that on unmodified supports. It was also expected that the active sites in the methane combustion, which are suspected to be PdO, were influenced by the acidic properties of the support.

DOI: 10.1134/S002315841004021X

INTRODUCTION

The catalytic combustion of methane has been attracted much attention for many reasons. It was shown that this reaction is effective in producing energy in gas turbine combustors, while reducing pollutants emissions, and in the elimination of trace of volatile organic compounds included in the exhaust gas, which cause the severe greenhouse effect [1–5].

Palladium is the most active catalyst in the total oxidation of methane among transition metal [6–9]. It was shown that the different oxidation states of palladium species can have different catalytic properties in this reaction [10]. Furthermore, it has been revealed that the active Pd species depends remarkably on the reaction conditions and the kind of supports. In fact, the role of the support is too important insofar the crystal structure, the nature of the surface and the acid-base character of support possibly affected the catalysis of Pd [11–14]. That is to say, the properties of supported Pd such as dispersion, particle size and oxidation state are greatly influenced by the acid-base and textural properties of the support.

The zeolite-supported Pd catalysts are paid considerable attention due to their excellent low temperature activity and high conversion efficiency and durability for methane combustion [15–17]. In fact, zeolite is an especially suitable material for the investigation of the support effect on Pd activity, because it is easy to control, on the one hand the amount and the strength of acid sites, and on the other hand the texture and structure through changing the Al concentration by dealumination.

Therefore, the dealumination, additionally to its influence on the acidity, texture and structure of the support, leads to the improvement of the hydrothermal stability of the support [17], which is a very important parameter in this reaction. Insofar, Shi et al. [18] have advanced that as zeolite-supported Pd catalysts are typically prepared by an ion-exchange method and consequently show a poor thermal and hydrothermal stability due to the sintering of palladium in the steam, which is a serious concern for the development of these materials for practical purposes.

Furthermore, it is reported that the main methods of dealumination can be divided into three groups: hydrothermal treatment [19, 20], acid treatment [21, 22] and dealumination by silicate derivatives such as $(NH_4)_2SiF_6$ or $SiCl_4$ [23, 24]. However, the latter treatment does not create secondary porosity [25], unlike the two others that contributes to the generation of secondary pores with wider distribution in the micro- or mesopore region in addition to the zeolitic primary pores regularly arrayed in the micropore region [26]. Therefore, formations of mesopores as well as dealumination are critical for improving the catalytic performance of HY-zeolites. Especially since mesoporous support are suitable for metals and metal oxide providing catalysts with quite interesting activity in several catalytic process [27].

Our final aim is to study the catalytic activity of palladium loaded on dealuminated zeolitic support in the catalytic combustion of methane. For this purpose, dealumination treatments using HNO_3, HCl, and H_2SiF_6 were applied to the Y-support then exchanged with palladium following the aqueous ion-exchange method. Structural characterization of final sample was carried out by means of X-ray diffraction and the

[1] The article is published in the original.

Table 1. Catalysts preparation

Symbols of samples	Treating reagent	Concentration, mol/l	Treatment time, h	Treatment temperature, °C
PdY1	HCl	0.05	24	ambient
PdY2	HCl	0.1	24	ambient
PdY3	HNO_3	0.05	4	80
PdY4	HNO_3	0.1	4	80
PdY5	H_2SiF_6	0.05	4	70

analyses of the textural properties were combined with the spectroscopic analysis by UV-visible spectroscopy. The metallic dispersion on zeolitic support was determined using hydrogen chimisorption.

EXPERIMENTAL

Catalysts Preparation

HY-zeolite was obtained by a successive ion exchange of the zeolite NaY (Zeolyst corp. 2.4) in a 0.1 M aqueous solution of NH_4Cl, followed by calcination at 773 K for 12 h. The obtained HY zeolite was dealuminated by using acid solutions as shown in Table 1. The support used for the preparation of catalysts was microporous with the pore diameter $d < 20$ Å. Pd-containing samples (1 wt % of Pd) were prepared by ion exchange of HY (1 g) with 0.1 ml of aqueous solution of $Pd(NH_3)_4Cl_2$ (Engelhart). After stirring of 24 h at room temperature the obtained PdY-samples was filtered, washed with distillate water and finally dried at 353 K.

The obtained catalysts were finally calcined at 773 K under an oxygen flow (30 cm^3/min) during 12 h.

Catalysts Characterization

The UV-visible absorption spectra of the prepared catalysts were obtained in spectrophotometer Perkin Elmer Lambda 45 equipped with a photodiode detector. The samples analysis was carried out in diffuse reflection under ambient atmosphere in the field 200–800 nm.

The FT-IR measurements were recorded with a Perkin Elmer PRAGON 1000 PC spectrophotometer with a 2 cm^{-1} resolution. For these measurements, samples were diluted in KBr then pressed. The analysis is recorded in the field 400–3700 cm^{-1}. The Si/Al ratio of the dealuminated support is estimated by the empirically correlation equation using the frequency shift of the IR band in the framework vibration region for Na-type faujasite [28]:

$$x = (1 + \mathrm{Si/Al})^{-1} = 3.857 - 0.00621 w_{DR}$$
$$= 4.766 - 0.00439 w_{TOT}\ \mathrm{cm}^{-1},$$

where w_{DR} and w_{TOT} are respectively the double ring and asymmetrical valence (Table 2).

Porosity and surface area (S_{BET}) were determined by means nitrogen adsorption–desorption at 77 K using a Micromeritics Asap 2000 apparatus. Each sample was previously degassed at 523 K under a vacuum for 9 h. Specific total surface areas were calculated using the BET equation (Table 3).

Palladium dispersion in the catalysts (D, in %) was estimated by hydrogen chemisorption on the metal (Table 3). The measurements of hydrogen chemisorption were followed by gas chromatography. Each sample was previously reduced under hydrogen in dynamic mode and raising the temperature up to 573 K at 5 K/min, then kept at this temperature for 30 min. The sample was then swept under nitrogen flow during 40 min at 593 K. After cooling of the cell containing the sample to room temperature, a mixture of hydrogen and nitrogen with a volume ratio 1 : 4 and a total flow of 50 cm^3/min was sent on the sample. The measurements of the adsorbed hydrogen quantity can then determine the dispersion of palladium.

$$D = \frac{N_{Pd}^{s}}{N_{Pd}^{t}} \times 100.$$

Here, N_{Pd}^{s} represents the molar number of the palladium in the surface, calculated from the volume of H_2 chimisorbed; N_{Pd}^{t}, the total molar number of the palladium.

Furthermore, the average palladium particles diameter (in Å) was also calculated from the dispersion

Table 2. The frequency shift w_{DR} and w_{TOT} and the Si/Al ratio estimated from IR results

Samples	w_{DR}	w_{TOT}	Si/Al ratio	
			w_{DR}	w_{TOT}
PdHY	–	–	2.4	2.4
PdY1	577	1050	2.65	5.39
PdY2	576	1031	2.57	3.17
PdY3	582	1051	3.12	5.57
PdY4	580	1038	2.92	3.78
PdY5	576	1020	2.57	2.47

Table 3. Palladium dispersion (D), diameter of palladium particles (d), surface area (S_{BET}) and porous volumes (total and meso) of different samples

Samples	D, %	d, Å	S_{BET}, m^2/g	V_{pore}, cm^3/g	
				total	meso*
PdHY	29	39.90	556	0.33	0.04
PdY1	15	77.13	194	0.17	0.08
PdY2	35	33.06	321	0.22	0.06
PdY3	15	77.13	120	0.13	0.08
PdY4	38	30.45	306	0.21	0.07
PdY5	40	28.92	534	0.32	0.05

* The mesopore volume was estimated from the following equation [36]: $V_{meso} = V_{total} - V_{micro}$.

Table 4. Chemical composition of the prepared samples determined by chemical analysis

Samples	Composition, %				
	Pd	Al	Si	Na	Si/Al_{TOT}
PdHY	1.19	9.47	21.87	5.73	2.42
PdY1	0.96	9.15	33.65	0.96	3.83
PdY2	1.16	10.41	27.39	1.39	2.74
PdY3	1.12	9.79	28.74	0.91	3.06
PdY4	1.32	10.29	26.64	1.19	2.7
PdY5	1.09	8.69	23.17	5.90	2.8

measurements by using the theoretical expression (assuming spherical particles) [29]:

$$d = \frac{1157}{D}.$$

The quantity of palladium exchanged and the total Si/Al ratios of different support are determined by the wet chemically analysis (Table 3).

The TPR experiments were carried out in a conventional apparatus using an H_2/Ar mixture (3% H_2). Catalysts samples of 50 mg were packed in a glass tube and pretreated in a flow of air at 773 K for 1 h. After calcination treatment, the samples were purged under a flow of argon and then cooled to 323 K. The TPR profiles were obtained in the 323–773 K temperature range with a heating rate of 10 K/min at a constant flow rate of 15 cm^3/min.

Catalytic Test

Methane combustion was carried out in a conventional flow unit with a fixed bed reactor using 60 mg of the sample. A gas reacting mixture of methane diluted with O_2 and He in the respective proportion of 1 : 4 : 95 and total flow rate of 6 l/h was fed into a Pyrex glass reactor under atmospheric pressure. Before each experiment, catalyst was reactivated with O_2 flux (4 ml/min) at 773 K. Reaction products were analyzed in a gas chromatograph equipped with a thermal conductivity detector. The activities were evaluated between 573 and 773 K; under these conditions the reaction is completely selective towards CO_2. It is important to note that the catalyst's particle size used for methane oxidation, after calcination at 500°C was esteemed to 2 nm [10].

RESULTS AND DISCUSSION

IR and UV-Visible Spectroscopy

The Si/Al ratios determined using the IR study results are summarized in Table 2. The value obtained for PdHY was 2.4, which agreed well with 2.42, the Si/Al ratio calculated from the results of chemical analysis shown in Table 4. Furthermore, as shown from IR measurements, there is an increase in the Si/Al ratio of the zeolite framework reaching 3.12 (using w_{DR}) and 5.57 (using w_{TOT}). This increase evolves according to the nature and the concentration of the dealuminated agent. In fact, dealumination by HNO_3 leads to a noticeable raise in the Si/Al ratio. This is can directly be seen by the shift of w_{DR} in the IR spectra (Fig. 1). Moreover, changes of the spectra shapes are observed after support dealumination concerning the bending, symmetrical and asymmetrical stretching vibrations of the T–O–T (T = Si or Al) units at 572, 720–780, and 1012–1160 cm^{-1}, respectively. This result suggests that aluminium atoms are removed from the framework [26]. In fact, the study by IR can inform on the structural changes of zeolite insofar as a proportion of broken up is notably observable on dealuminated samples. Moreover, the shape of the peaks become broader suggesting a higher non-uniform distribution of the Si/Al ratios of the framework or a higher amount of defect sites as described by Salman et al. [30]. In fact, the IR spectra of treated samples with acids (0.1 M), shows a remarkably shift in w_{TOT} indicating that samples already contains a significant portion of decomposed framework. This observation is confirmed by the studies of Lutz et al. [31].

In addition, Fig. 2 represents UV-visible spectra of the various samples treated under oxidizing atmosphere at 773 K. The majority of the authors consider that in UV-visible spectra, the ionic states of palladium can be identified; otherwise metal Pd^0 characterized by absorption without a defined structure in all range of the spectrum [32]. In fact, the spectra of the catalysts show absorption bands at 214, 430–450 nm and a shoulder towards 310 nm. The first one is due to a zeolite reflexion and corresponds to that observed by Garbowski [33]. The second band corresponds to the d–d electronic transitions assigned to Pd^{2+} [32, 34]. The shoulder observed is allotted to a charge transfer of the oxygen ligands towards metal in sites $O^{2-} \rightarrow Pd^{2+}$. These sites resulted from the substitution of NH_3

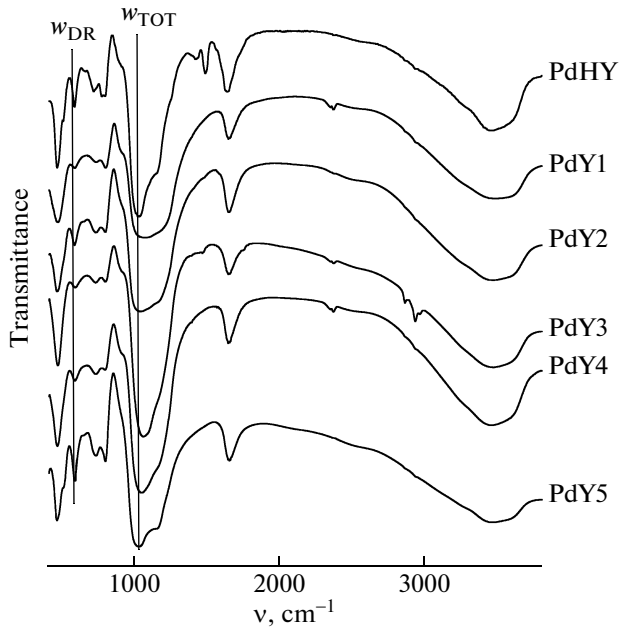

Fig. 1. Infrared spectra of PdHY and samples prepared with dealuminated zeolite.

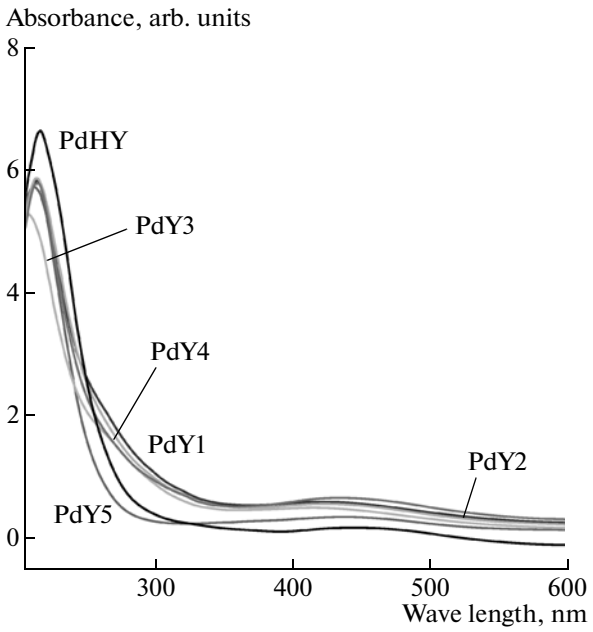

Fig. 2. UV-visible spectra of PdHY and samples prepared with dealuminated support.

ligands by oxygen ligands of the zeolitic support after the decomposition of the complex $[Pd(NH_3)_4]^{2+}$ [35]. Besides, signals at 250–260 and 410–420 nm are attributed to highly dispersed PdO particles [36].

Pd Dispersion and Textural Measurements

The determination of the metal dispersion (Table 3) revealed that the palladium species are well dispersed on support dealuminated by acids with a low concentration. This observation implies that the structure properties affect the metal distribution on the zeolitic support surface. Furthermore, low palladium dispersion is recorded for PdY1 and PdY3 while the protons of the support are easy to exchange with palladium. In fact, it is known that the zeolite protons lead to stabilization of small Pd particles for the ion-exchange catalysts [37]. The obtained result can be explained by the fact that there is an electron transfer from the metal to acid sites and, consequently, the chemisorption ability of the Pd particles is inhibited [37]. Additionally, the low metallic dispersion can be explicated by the formation of the amorphous phase, which blocks the zeolite pores and decrease the palladium exchange sites. However, these results probably suggest that PdO species could be formed on PdY1 and PdY3 [18].

Thus the dispersion results (Table 3) were in accordance with the metal particles size. Sachtler and Zhang [38] explain this fact by the reduction of the acid site density at higher Si/Al values.

Moreover, values of surface area, porous and mesoporous volume of samples are also included in Table 3. Interestingly, it must be pointed out that the textural properties of samples dealuminated with acids 0.1 M were severely affected, probably due to the collapse of the crystalline structure and to the partial blockage of the zeolite pore system. Such modifications are accompanied by a development of a secondary mesoporous system [39] which is more important in the case of the samples dealuminated by acids 0.1 M than samples treated with acids 0.05 M (Fig. 3). This result is in agreement with IR spectroscopy measurements revealing the structural changes of these samples. In fact, according to N_2 adsorption–desorption, the porous character of the dealuminated samples was largely dependent on the nature and the concentration of the acid used for the dealumination treatment. Therefore, these observations explain the various shapes of the adsorption–desorption isotherms (Fig. 3). It is clear that for sample dealuminated with H_2SiF_6 (0.05 M), comparing to the other dealuminated samples, with no hysteresis loop, corresponds perfectly to type I in the Brunauer classification, which is typical for the crystalline microporous materials. Furthermore, similar surface area values were obtained for PdHY and PdY5. This leads to note that for this sample the microporous character is largely retained.

TPR Results

Thus, H_2-TPR was used to characterize the reducibility of the palladium species which could be an important factor for the catalytic oxidation reactions. The TPR profiles of the samples of PdY catalysts are shown in Fig. 4. According to the literature [40, 41],

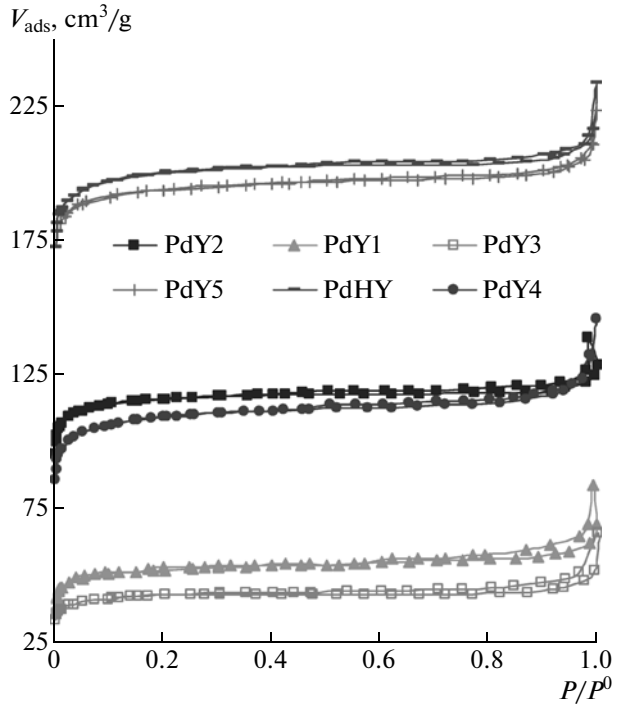

Fig. 3. N_2 adsorption–desorption isotherms of various samples at 77 K.

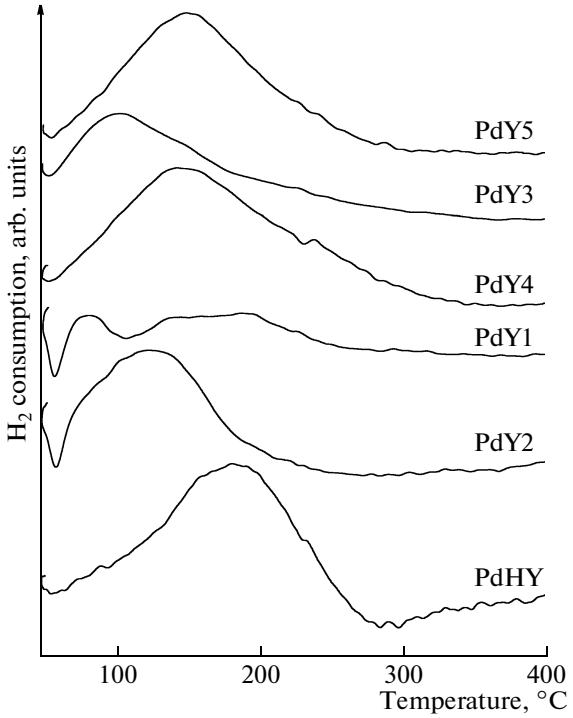

Fig. 4. TPR profiles of the PdY catalysts.

the hydrogen consumed indicates the reduction of PdO to metallic Pd. It is important to notice that the low temperature peaks in these profiles are clearly due to the reduction of palladium oxide crystals.

As shown in Fig. 4, a reduction peak was observed at 180°C for PdHY, and it shifted to low temperature for other samples. Maeda and al. [7] contribute this shift to the increase of the Si/Al molar ratio of the zeolite.

The sharp peak was observed on these samples except on PdY1 where the peak was broad and double-spiked. Thus, a high dispersion of palladium in the zeolite was estimated [7].

Catalytic Test

The activities of catalysts are followed during about 3 h. Figure 5 illustrates the carves representing the conversion of methane versus time for the reaction carried out at 773 K in the presence of various catalysts. It is clear that all samples reach a steady state after approximately 1.5 h. Furthermore, it is revealed that the highest conversion of methane (76%) is obtained in the presence of catalyst prepared with dealuminated zeolite by HNO_3 (0.1 M). Moreover, even with PdY4, a relatively high conversion rate (70%) is recorded. The behavior of these catalysts in the methane combustion reaction is probably relied to the presence of the second porosity. This result let us suggesting that this reaction depends on the textural properties of the support. The change of the Si/Al ratio can also affect the methane conversion. In fact, we observe an enhancement in the methane conversion rate when increasing Si/Al ratio of the support. On the other hand, according to the chimisorption results, the active sites on catalysts prepared with dealuminated supports with acids (0.1 M) are perhaps PdO. In fact, many authors consider that PdO is an active component for methane combustion in the oxygen-rich conditions [42, 43].

The results of the test giving the conversion of methane according to the temperature are represented on Fig. 6. It is shown that all the samples are practically inactive at a temperature lower than 573 K. Moreover, the PdY3 seems to be the most active catalyst in the entire temperature range studied. However, the low methane conversion is obtained in the presence of PdY5. Besides, it is observed that the sample PdY4 is activated slowly according to the temperature until 698 K, comparing to the other catalysts, after this temperature there are an enhancement in its activity.

The catalytic performances of samples as the function of the temperature are also evaluated by the determination of the temperatures of isoconversion T_{10} and T_{50} corresponding to the conversion rates 10 and 50% respectively (Table 5). Furthermore, while basing on these results, it is confirmed that PdY1 and PdY5 are activated slowly according to the temperature. In fact, since to reach the methane conversion rate 10% it is necessary for these catalysts a rather high temperature. However, the behavior of the catalysts prepared with

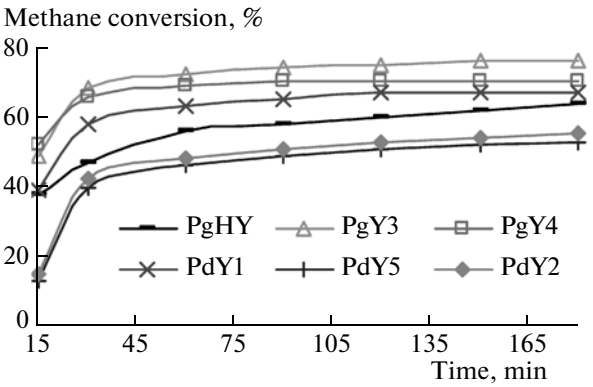

Fig. 5. Methane conversion on various catalysts at 773 K versus time of reaction.

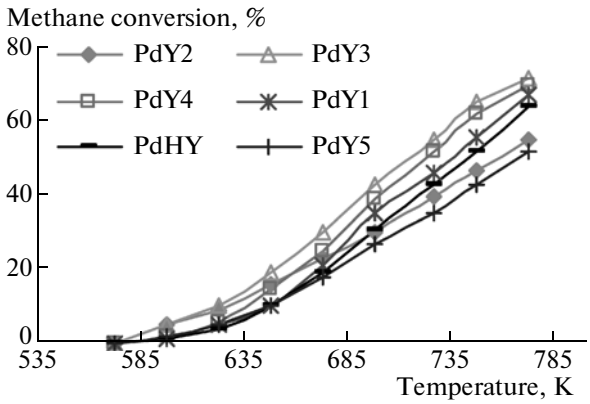

Fig. 6. Methane conversion on various catalysts versus temperature of reaction.

delaminating acids 0.05 M excepting by the acid H_2SiF_6, as a function of the temperature, seems to be different.

Moreover, the activity of palladium in the reaction of methane combustion is greatly dependent on the nature and the concentration of the dealuminated agent. Specially, as it is seen from Table 5, since the exchange rate of palladium is virtually the same for different samples and it is in agreement with the theoretical rate (1%).

In fact, it is shown that the support dealumination with HNO_3 promoted to the improvement of the methane conversion rate. Interestingly, it must be pointed out that, in addition to the texture properties, the support acidity would have probably a large influence on the activity of palladium in this reaction. Indeed, the dealumination of zeolites modifies besides the pore structures, entails change in Br0nsted and Lewis acid sites [44–46]. As it is known in the literature, the active centres of zeolites are Brønsted acid sites formed by bridging OH groups [47]. After dealumination, the aluminium removed from the framework remains in the cavities as nanoparticles whose surfaces possess Lewis acidity [45, 46]. These Lewis sites may have their own catalytic activity or may interact with Brønsted sites, inducing an increase in acid strength and thus a modification of catalytic activity [48]. It was suggested by Okumura et al. [11] that the higher acid strength of H-MOR played a role in keeping the higher dispersion of PdO on H-MOR than on H-MFI, because the acid–base interaction was considered to be the driving force for anchoring of PdO. As it is expected that PdO are the active sites in the reaction of methane combustion, this possibly confirms the fact that zeolite acidity affect the palladium activity. Additionally, M'Ramadj et al. [49] found that Pd catalysts supported on ZSM-5 with both Brønsted and Lewis sites have better activity than Pd catalyst supported on Al_2O_3, where no Brønsted sites are present. They concluded that the activation of methane and the catalytic performance was related to the surface acidity of catalysts.

On the other hand, the activity of Pd supported on dealuminated zeolite is dependent on the concentration of aluminium atoms as described by Maeda et al. [7]. On the basis of these results, it is plausible to advance that the Si/Al ratio can affect the catalytic performances of zeolite supported palladium catalysts toward combustion of methane. Insofar, as the change of this ratio influences the concentration of the aluminium atoms and, as a consequence, the acid properties of the support.

Thus, the support effect of zeolite on the methane combustion activity of Pd was studied. It is found that the support dealumination by acids can greatly affect the activity of Pd. In fact, it was observed that there is improvement in the methane conversion when rising Si/Al ratio of zeolite. Moreover, it is important to note that the presence of the secondary porosity in the zeolitic support has a considerable effect on the activity of Pd in the methane combustion. Additionally, the results reported above indicate that methane oxidation rates were affected greatly by acid sites properties of catalyst, which are modified after he dealumination. Furthermore, it may be suggested that the zeolite characteristics changed after the dealumination, can influence in the interaction of active sites-support as well as their dispersion and therefore, their activity.

Table 5. Temperatures corresponding to the conversion rates 10 and 50% on the different catalysts

Isoconversion temperature, K	Sample					
	PdHY	PdY1	PdY2	PdY3	PdY4	PdY5
T_{10}	645	648	628	623	635	648
T_{50}	735	735	757	714	723	768

REFERENCES

1. Liu, C.J., Yu, K., Zhang, Y.P., Zhu, X., He, F., and Eliasson, B., *Appl. Catal., B*, 2004, vol. 47, p. 95.
2. Choudhary, T.V., Banerjeeand, S., and Choudhary, V.R., *Appl. Catal., A*, 2002, vol. 234, p. 1.
3. Truitt, M.J., Toporek, S.S., Rovira-Hernandez, R., Hatcher, K., and White, J.L., *J. Am. Chem. Soc.*, 2004, vol. 126, p. 11 144.
4. Gelin, P. and Primet, M., *Appl. Catal., B*, 2002, vol. 39, p. 1.
5. Wang, C.B., Ho, C.M., Lin, H.K., and Chiu, H.C., *Fuel*, 2002, vol. 81, p. 1883.
6. Li, Y. and Armor, J.N., *Appl. Catal., B*, 1994, vol. 3, p. 275.
7. Maeda, H., Kinoshita, Y., Reddy, K.R., Muto, K., Komai, S., Katada, N., and Niwa, M., *Appl. Catal., A*, 1997, vol. 163, p. 59.
8. Okumura, K., Shinohara, E., and Niwa, M., *Catal. Today*, 2006, vol. 117, p. 577.
9. Ruiz, J.A.C., Fraga, M.A., and Pastore, H.O., *Appl. Catal., B*, 2007, vol. 76, p. 115.
10. Said, Zina M. and Ghorbel, A., *Solid State Sci.*, 2004, vol. 6, p. 973.
11. Okumura, K., Matsumoto, S., Nishiaki, N., and Niwa, M., *Appl. Catal., B*, 2003, vol. 40, p. 151.
12. Muto, K., Katada, N., and Niwa, M., *Appl. Catal., A*, 1996, vol. 134, p. 203.
13. Okumura, K., Tanaka, H., and Niwa, M., *Catal. Lett.*, 1999, vol. 58, p. 43.
14. Ozawa, Y., Tochihara, Y., Watanabe, A., Nagai, M., and Omi, S., *Appl. Catal., A*, 2004, vol. 258, p. 261.
15. Choudhary, V.R., Uphade, B.S., and Pataskar, S.G., *Fuel*, 1999, vol. 78, p. 919.
16. Wang, C.B., Ho, C.M., Lin, H.K., and Chiu, H.C., *Fuel,* 2002, vol. 81, p. 1883.
17. Beyer, H.K., *Dealumination Techniques for Zeolites (Molecular Sieves)*, Berlin: Springer, 2002.
18. Shi, C., Yang, L., and Cai, J., *Fuel*, 2007, vol. 86, p. 106.
19. Dimitrijevic, R., Lutz, W., and Ritzmann, A., *J. Phys. Chem. Solids*, 2006, vol. 67, p. 1741.
20. Hamid, S.H. and Ashraf Sli, M., *Handbook of MTBE and Other Gasoline Oxygenates*, New York: Marcel Dekker, 2004.
21. Gola, A., Rebours, B., Milazzo, E., Lynch, J., Benazzi, E., Lacombe, S., Delevoye, L., and Fernandez, C., *Microporous Mesoporous Mater.*, 2000, vol. 40, p. 73.
22. Yan, Z., Ma, D., Zhuang, J., Liu, X., Han, X., Bao, X., Chang, F., Xu, L., and Liu, Z., *J. Mol. Catal. A: Chem.*, 2003, vol. 194, p. 153.
23. Pires, J., Carvalho, A., Pinto, M., and Rocha, J., *J. Porous Mater.*, 2006, vol. 13, p. 107.
24. Kao, H.M. and Chang, P.C., *J. Phys. Chem. B*, 2006, vol. 39, p. 19 104.
25. Akporiaye, D., Chapple, A.P., Clark, D.M., Dewyer, J., Elliot, I.S., and Rawlance, D.J., *"New Developments in Zeolite Sciences and Technology," Proc. 7th Int. Conf.*, Tokyo, 1987, p. 351.
26. Kawai, T. and Tsutsumi, K., *Adsorption*, 1998, vol. 4, p. 225.
27. Yuranov, I., Moeckli, P., Suvorova, E., Buffat, P., Kiwi-Minske, L., and Renken, A., *J. Mol. Catal. A: Chem.*, 2003, vol. 192, p. 239.
28. Sohn, J.R., Jong, R., De Canio, S.J., and Lunsford, J.H., *Appl. Spectrosc.*, 1986, vol. 6, p. 225.
29. Canaizares, P., De Lucas, A., Dorado, F., Duraan, A., and Asencio, I., *Appl. Catal., A*, 1998, vol. 169, p. 137.
30. Salman, N., Ruscher, C.H., Buhl, J.C., Lutz, W., Toufar, H., and Stocker, M., *Microporous Mesoporous Mater.*, 2006, vol. 90, p. 339.
31. Lutz, W., Rüscher, C.H., and Heidemann, D., *Microporous Mesoporous Mater.*, 2002, vol. 55, p. 193.
32. Pestryakov, A.N., Lunin, V.V., Fuentes, S., Bogdanchikova, N., and Barrera, A., *Chem. Phys. Lett.*, 2003, vol. 367, p. 102.
33. Garbowski, E.D., *J. Phys. Chem.*, 1978, vol. 75, p. 226.
34. Sass, A.S., Shvets, V.A., and Savelyeva, G.A., *Russ. J. Phys. Chem.*, 1986, vol. 60, p. 219.
35. Roldán, R., Beale, A.M., Sánchez-Sánchez, M., Romero-Salguero, F.J., Jiménez-Sanchidrián, C., Gómez, J.P., and Sankar, G., *J. Catal.*, 2008, vol. 254, p. 12.
36. Kravchuk, L.S., Stelmakh, E.I., and Ivashenko, N.I., *Kinet. Catal*, 1992, vol. 33, p. 618.
37. Janssen, A.H., Koster, A.J., and de Jong, K.P., *J. Phys. Chem. B*, 2002, vol. 106, p. 11 905.
38. Sachtler, W.M.H. and Zhang, Z., *Adv. Catal.,* 1993, vol. 39, p. 129.
39. Garralon, G., Fornes, V., and Corma, A., *Appl. Spectrosc.,* 1988, vol. 8, p. 268.
40. Homeyer, S.T. and Sachtler, W.M.H., *J. Catal.,* 1989, vol. 117, p. 91.
41. Shen, W.J., Okumura, M., Matsumura, Y., and Haruta, M., *Appl. Catal., A*, 2001, vol. 213, p. 225.
42. Hicks, R.F., Qi, H., Young, M.L., and Lee, R.G., *J. Catal.*, 1990, vol. 122, p. 280.
43. Briot, P. and Primet, M., *Appl. Catal.,* 1991, vol. 68, p. 301.
44. McQueen, D., Chiche, B.H., Fajula, F., Auroux, A., Guimon, C., Fitoussi, F., and Schulz, P., *J. Catal.,* 1996, vol. 161, p. 587.
45. Boreave, A., Auroux, A., and Guimon, C., *Microporous Mater.,* 1997, vol. 11, p. 275.
46. Lonyi, F., Vaylon, J., and Pal-Borbely, G., *Microporous Mesoporous Mater.*, 2003, vol. 66, p. 273.
47. Tao, Y., Kanoh, H., Abrams, L., and Kaneko, K., *Chem. Rev.,* 2006, vol. 106, p. 896.
48. Yong, Y., Gruver, V., and Fripiat, J.J., *J. Catal.,* 1994, vol. 150, p. 421.
49. M'Ramadj, O., Li, D., Wang, X., Zhang, B., and Lu, G., *Catal. Commun.,* 2007, no. 8, p. 880.